Perspectives of quantum plasma and warm dense matter theory[1]

Michael Bonitz, Zhandos Moldabekov[**], Tobias Dornheim[†], Paul Hamann, Jan Vorberger[*]

in collaboration with Alexey Filinov, Travis Sjostrom[1], Fionn D. Malone[2], W.M.C. Foulkes[3], and Frank Graziani[2]

Institute of Theoretical Physics and Astrophysics, Kiel University
[†] Center for Advanced Systems Understanding, [*] Helmholtz-Zentrum Dresden
[**] Al Farabi University, Almaty, Kazakhstan

[1] Theoretical Division Los Alamos National Laboratory, Los Alamos, New Mexico, USA
[2] Lawrence Livermore National Lab
[3] Department of Physics, Imperial College London, UK

September 2020

[1] http://www.theo-physik.uni-kiel.de/bonitz/index.html ⇒ Research ⇒ Publications, Talks

Introduction: warm dense matter

Warm dense matter (WDM):

- Nearly classical ions
- Degenerate non-ideal electrons
- Coupling parameter:

$$r_s = \frac{\bar{r}}{a_{\mathrm{B}}} \sim 0.1 \ldots 10$$

- Degeneracy parameter:

$$\theta = T/T_{\mathrm{F}} \sim 0.1 \ldots 10$$

- Temperature, degeneracy and coupling effects equally important
  $\rightarrow$ No small parameters

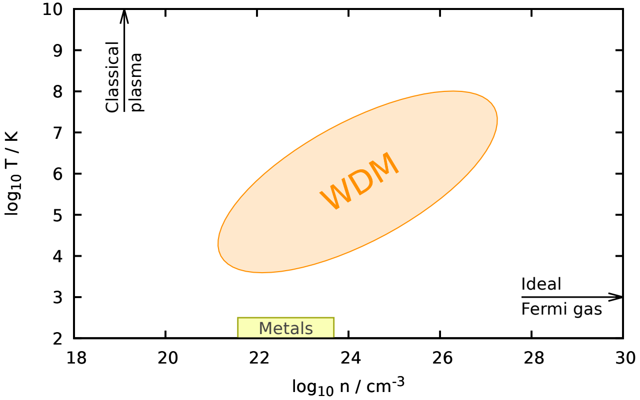

Figure: From T. Dornheim, S. Groth, and M. Bonitz, *Physics Reports* **744**, 1-86 (2018)

Perturbation theory and ground-state approaches fail

Importance of the uniform electron gas (UEG)

Model system of Coulomb interacting quantum electrons in a uniform positive background

Ground state ($T = 0$):

- Simple model for conduction electrons in metals
- **Exchange-correlation (XC) energy**:

$$e_{xc}(r_s) = e_{tot}(r_s) - e_0(r_s)$$

$\rightarrow$ Input for density functional theory (DFT) simulations (in LDA and GGA)
$\rightarrow$ Parametrization[1] of $e_{xc}(r_s)$ from ground state quantum Monte Carlo data[2]

[1] J.P. Perdew and A. Zunger, PRB **23**, 5048 (1981) [2] D.M. Ceperley and B. Alder, PRL **45**, 566 (1980) [3] N.D. Mermin, Phys. Rev **137**, A1441 (1965)
[4] A.Y. Potekhin and G. Chabrier, *A&A **550**, A43* (2013)

Importance of the uniform electron gas (UEG)

Model system of Coulomb interacting quantum electrons in a uniform positive background

Ground state $(T = 0)$:

- Simple model for conduction electrons in metals
- **Exchange-correlation (XC) energy**:

$$e_{xc}(r_s) = e_{tot}(r_s) - e_0(r_s)$$

→ Input for density functional theory (DFT) simulations (in LDA and GGA)
→ Parametrization[1] of $e_{xc}(r_s)$ from ground state quantum Monte Carlo data[2]

Warm dense matter $(T \sim T_F)$:

- **Thermal DFT**[3]: minimize free energy $F = E - TS$
  → Requires parametrization of XC **free** energy of UEG:

$$f_{xc}(r_s, \theta) = f_{tot}(r_s, \theta) - f_0(r_s, \theta)$$

- $f_{xc}(r_s, \theta)$ direct input for **EOS models** of astrophysical objects[4]
- $f_{xc}(r_s, \theta)$ contains **complete thermodynamic information** of UEG

---

1 J.P. Perdew and A. Zunger, PRB **23**, 5048 (1981) 2 D.M. Ceperley and B. Alder, PRL **45**, 566 (1980) 3 N.D. Mermin, Phys. Rev **137**, A1441 (1965)
4 A.Y. Potekhin and G. Chabrier, *A&A* ***550****, A43* (2013)

Many parametrizations for f_{xc} based on different approximate approaches:

- Semi-analytical approaches by **Ebeling**[1]
- Dielectric methods, e.g. Singwi-Tosi-Land-Sjölander[2] (**STLS**) and Vashista-Singwi[3] (**VS**)
- Quantum-classical mappings, e.g. Perrot and Dharma-wardana[4] (**PDW**)
- **Most recent:** Fit by Karasiev[5] *et al.* (**KSDT**) to Restricted Path Integral Monte Carlo (**RPIMC**) data[6]

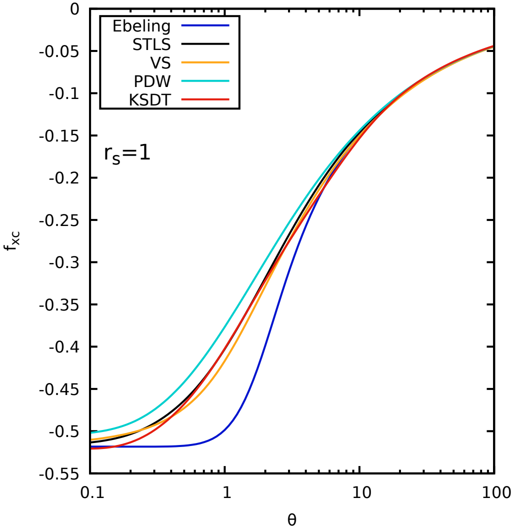

[1] W. Ebeling and H. Lehmann, Ann. Phys. **45**, (1988)
[2] S. Ichimaru, H. Iyetomi, and S. Tanaka, Phys. Rep. **149**, (1987)
[3] T. Sjostrom and J. Dufty, PRB **88**, (2013)
[4] F. Perrot and MWC Dharma-wardana, PRB **62**, (2000)
[5] V.V. Karasiev *et al.*, PRL **112**, (2014)
[6] E.W. Brown *et al.*, PRL **110**, (2013)

Many parametrizations for f_{xc} based on different approximate approaches:

- Semi-ana
- Dielectric
  (**STLS**) a
- Quantum-classical mappings, e.g. Perrot and Dharma-wardana[4] (**PDW**)
- **Most recent:** Fit by Karasiev[5] *et al.* (**KSDT**) to Restricted Path Integral Monte Carlo (**RPIMC**) data[6]

Goal: obtain *ab initio* parametrization of $f_{xc}(r_s, \theta)$

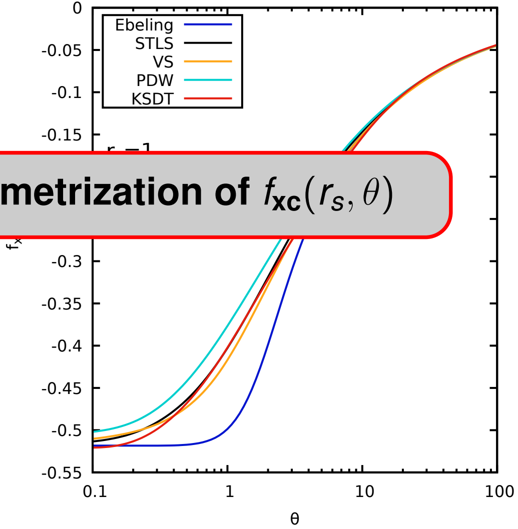

---

[1] W. Ebeling and H. Lehmann, Ann. Phys. **45**, (1988)
[2] S. Ichimaru, H. Iyetomi, and S. Tanaka, Phys. Rep. **149**, (1987)
[3] T. Sjostrom and J. Dufty, PRB **88**, (2013)
[4] F. Perrot and MWC Dharma-wardana, PRB **62**, (2000)
[5] V.V. Karasiev *et al.*, PRL **112**, (2014)
[6] E.W. Brown *et al.*, PRL **110**, (2013)

Path integral Monte Carlo (PIMC) simulation of the warm dense UEG

- Standard PIMC in warm dense regime severely hampered by ***fermion sign problem***:

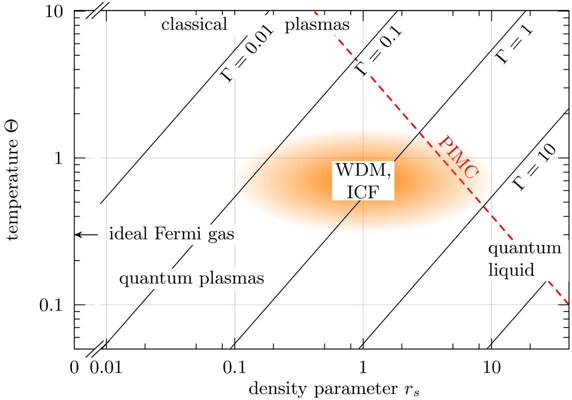

[1] E.W. Brown *et al.*, PRL **110**, 146405 (2013) [2] T. Schoof *et al.*, Phys. Rev. Lett **115**, 130402 (2015) [3] T. Schoof *et al.*, Contrib. Plasma Phys. **51**, 687 (2011)
[4] T. Dornheim *et al.*, New J. Phys. **17**, 073017 (2015) [5] T. Dornheim *et al.*, J. Chem. Phys. **143**, 204101 (2015)

Path integral Monte Carlo (PIMC) simulation of the warm dense UEG

- Standard PIMC in warm dense regime severely hampered by ***fermion sign problem***:
  - First results[1] by E. Brown, D. Ceperley *et al.* (2013) based on ***fixed node approximation*** (**RPIMC**)
  - Induces **systematic errors** of unknown magnitude
  - **RPIMC** limited to $r_s \gtrsim 1$

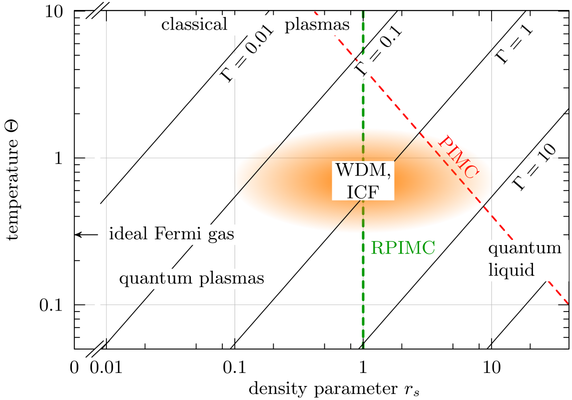

[1] E.W. Brown *et al.*, PRL **110**, 146405 (2013)
[2] T. Schoof *et al.*, Phys. Rev. Lett **115**, 130402 (2015)
[3] T. Schoof *et al.*, Contrib. Plasma Phys. **51**, 687 (2011)
[4] T. Dornheim *et al.*, New J. Phys. **17**, 073017 (2015)
[5] T. Dornheim *et al.*, J. Chem. Phys. **143**, 204101 (2015)

Path integral Monte Carlo (PIMC) simulation of the warm dense UEG

- Standard PIMC in warm dense regime severely hampered by ***fermion sign problem***:
  - First results[1] by E. Brown, D. Ceperley *et al.* (2013) based on ***fixed node approximation*** (**RPIMC**)
  - Induces **systematic errors** of unknown magnitude
  - **RPIMC** limited to $r_s \gtrsim 1$

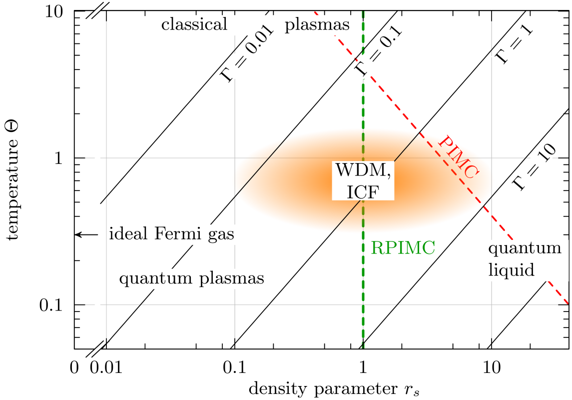

Our approach:

Avoid fermion sign problem by combining two exact and complementary QMC methods:

---

[1] E.W. Brown *et al.*, PRL **110**, 146405 (2013) [2] T. Schoof *et al.*, Phys. Rev. Lett **115**, 130402 (2015) [3] T. Schoof *et al.*, Contrib. Plasma Phys. **51**, 687 (2011)
[4] T. Dornheim *et al.*, New J. Phys. **17**, 073017 (2015) [5] T. Dornheim *et al.*, J. Chem. Phys. **143**, 204101 (2015)

Path integral Monte Carlo (PIMC) simulation of the warm dense UEG

- Standard PIMC in warm dense regime severely hampered by ***fermion sign problem***:
  - First results[1] by E. Brown, D. Ceperley *et al.* (2013) based on ***fixed node approximation*** (**RPIMC**)
  - Induces **systematic errors** of unknown magnitude
  - **RPIMC** limited to $r_s \gtrsim 1$

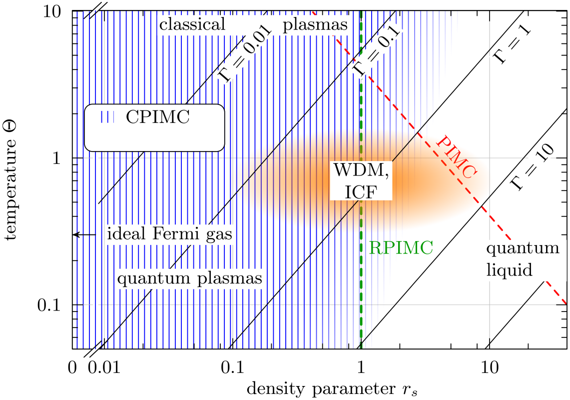

Our approach:

Avoid fermion sign problem by combining two exact and complementary QMC methods:

1. **Configuration PIMC (CPIMC)**[2,3]

$\rightarrow$ Excels at high density $r_s \lesssim 1$ and strong degeneracy

[1] E.W. Brown *et al.*, PRL **110**, 146405 (2013)
[2] T. Schoof *et al.*, Phys. Rev. Lett **115**, 130402 (2015)
[3] T. Schoof *et al.*, Contrib. Plasma Phys. **51**, 687 (2011)
[4] T. Dornheim *et al.*, New J. Phys. **17**, 073017 (2015)
[5] T. Dornheim *et al.*, J. Chem. Phys. **143**, 204101 (2015)

Path integral Monte Carlo (PIMC) simulation of the warm dense UEG

- Standard PIMC in warm dense regime severely hampered by ***fermion sign problem***:
  - First results[1] by E. Brown, D. Ceperley *et al.* (2013) based on ***fixed node approximation*** (**RPIMC**)
  - Induces **systematic errors** of unknown magnitude
  - **RPIMC** limited to $r_s \gtrsim 1$

Our approach:

Avoid fermion sign problem by combining two exact and complementary QMC methods:

1. **Configuration PIMC (CPIMC)**[2,3]

   → Excels at high density $r_s \lesssim 1$ and strong degeneracy
2. **Permutation blocking PIMC (PB-PIMC)**[4,5]

   → Extends standard PIMC towards stronger degeneracy

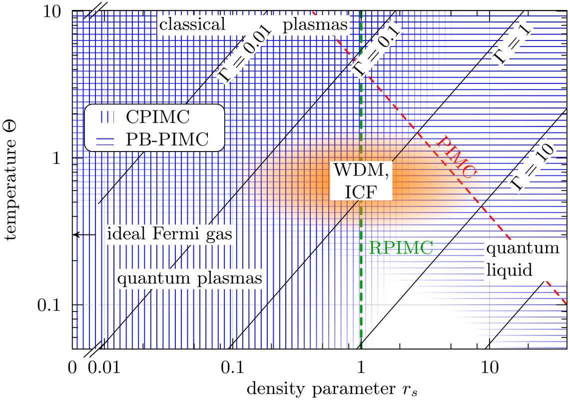

[1] E.W. Brown *et al.*, PRL **110**, 146405 (2013) [2] T. Schoof *et al.*, Phys. Rev. Lett **115**, 130402 (2015) [3] T. Schoof *et al.*, Contrib. Plasma Phys. **51**, 687 (2011)
[4] T. Dornheim *et al.*, New J. Phys. **17**, 073017 (2015) [5] T. Dornheim *et al.*, J. Chem. Phys. **143**, 204101 (2015)

Path integral Monte Carlo (PIMC) simulation of the warm dense UEG

- Standard PIMC in warm dense regime severely hampered by ***fermion sign problem***:
  - First results[1] by E. Brown, D. Ceperley *et al.* (2013) based on ***fixed node approximation*** (**RPIMC**)
  - Induces **systematic errors** of unknown magnitude
  - **RPIMC** limited to $r_s \gtrsim 1$

Our approach:

Avoid fermion sign problem by combining two exact and complementary QMC methods:

1. **Configuration PIMC (CPIMC)**[2,3]

   → Excels at high density $r_s \lesssim 1$ and strong degeneracy
2. **Permutation blocking PIMC (PB-PIMC)**[4,5]

   → Extends standard PIMC towards stronger degeneracy

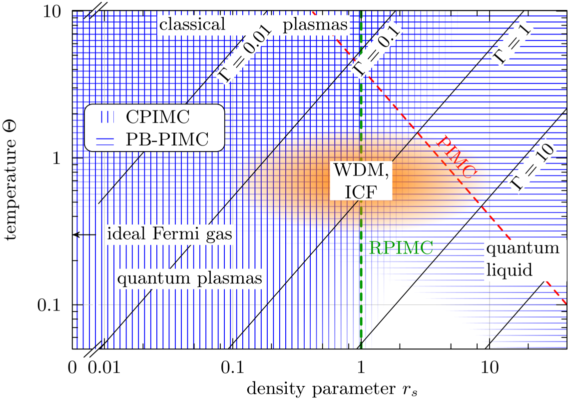

***Ab initio* simulations over broad range of parameters**

---

[1] E.W. Brown *et al.*, PRL **110**, 146405 (2013) [2] T. Schoof *et al.*, Phys. Rev. Lett **115**, 130402 (2015) [3] T. Schoof *et al.*, Contrib. Plasma Phys. **51**, 687 (2011)
[4] T. Dornheim *et al.*, New J. Phys. **17**, 073017 (2015) [5] T. Dornheim *et al.*, J. Chem. Phys. **143**, 204101 (2015)

Exact exchange-correlation energy $E_{xc} = E - E_0$ (E_0: ideal energy) ($N = 33$ spin-polarized electrons, $\theta \geq 0.5$, $\forall\ r_s$)

- **RPIMC** limited to $r_s \geq 1$

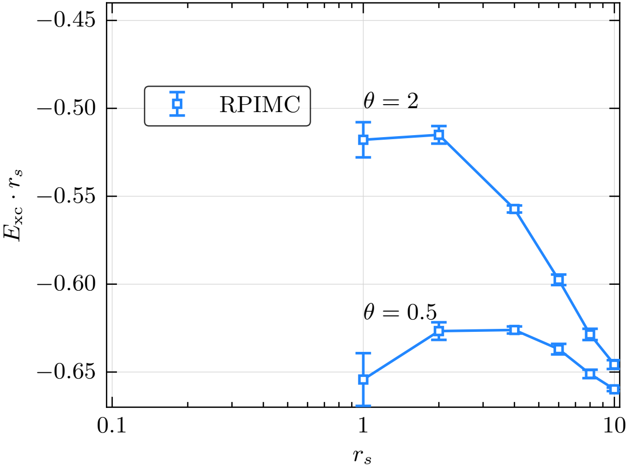

[1] S. Groth *et al.*, Phys. Rev. B **93**, 085102 (2016)
[2] T. Dornheim *et al.*, Phys. Rev. B **93**, 205134 (2016)
[3] F.D. Malone *et al.*, Phys. Rev. Lett. **117**, 115701 (2016)
[4] T. Schoof *et al.*, Phys. Rev. Lett. (2015)

Exact exchange-correlation energy $E_{xc} = E - E_0$ (E_0: ideal energy) ($N = 33$ spin-polarized electrons, $\theta \geq 0.5$, $\forall\ r_s$)

- **RPIMC** limited to $r_s \geq 1$
- **CPIMC** excels at high density

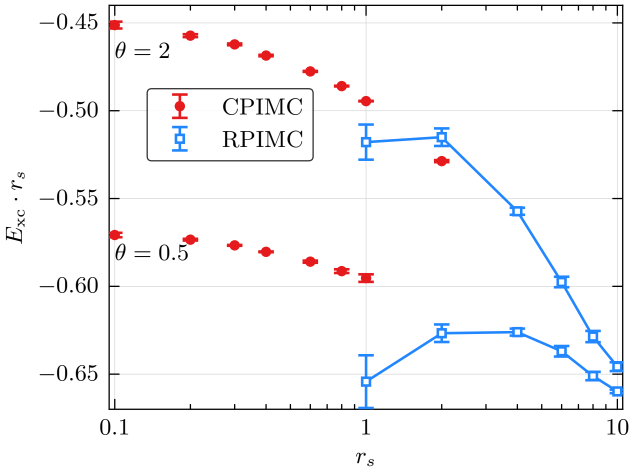

[1] S. Groth *et al.*, Phys. Rev. B **93**, 085102 (2016)
[2] T. Dornheim *et al.*, Phys. Rev. B **93**, 205134 (2016)
[3] F.D. Malone *et al.*, Phys. Rev. Lett. **117**, 115701 (2016)
[4] T. Schoof *et al.*, Phys. Rev. Lett. (2015)

Exact exchange-correlation energy $E_{xc} = E - E_0$ (E_0: ideal energy) ($N = 33$ spin-polarized electrons, $\theta \geq 0.5$, $\forall\, r_s$)

- **RPIMC** limited to $r_s \geq 1$
- **CPIMC** excels at high density
- **PB-PIMC** applicable at $\theta \gtrsim 0.5$

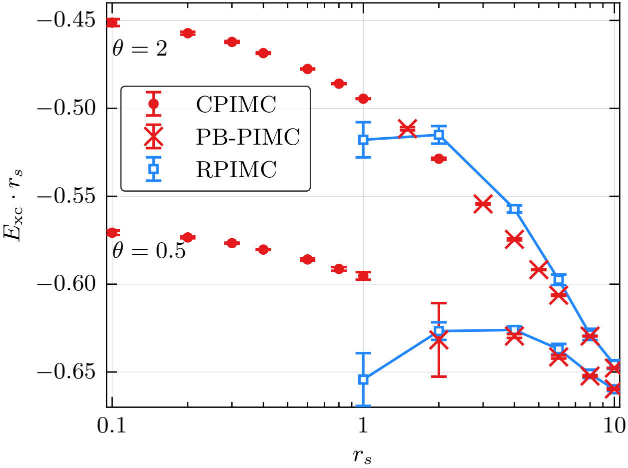

[1] S. Groth *et al.*, Phys. Rev. B **93**, 085102 (2016) [2] T. Dornheim *et al.*, Phys. Rev. B **93**, 205134 (2016)
[3] F.D. Malone *et al.*, Phys. Rev. Lett. **117**, 115701 (2016) [4] T. Schoof *et al.*, Phys. Rev. Lett. (2015)

Exact exchange-correlation energy $E_{xc} = E - E_0$ (E_0: ideal energy) ($N = 33$ spin-polarized electrons, $\theta \geq 0.5$, $\forall\ r_s$)

- **RPIMC** limited to $r_s \geq 1$
- **CPIMC** excels at high density
- **PB-PIMC** applicable at $\theta \gtrsim 0.5$

Combination[1] yields exact results over entire density range down to $\theta \sim 0.5$

- Also applies to the **unpolarized** UEG[2]
- confirmed by independent **DMQMC** simulations[3]

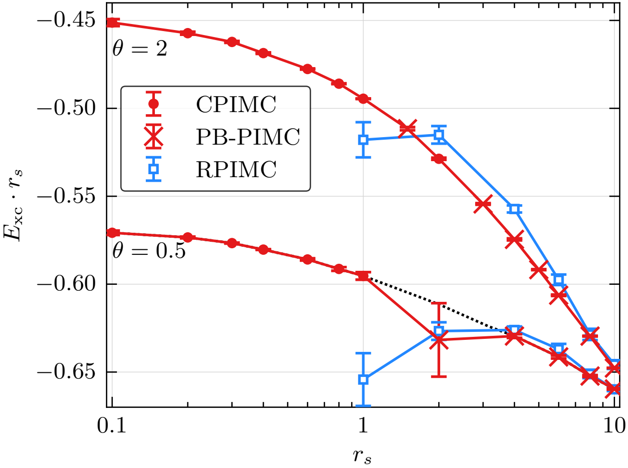

[1] S. Groth *et al.*, Phys. Rev. B **93**, 085102 (2016) [2] T. Dornheim *et al.*, Phys. Rev. B **93**, 205134 (2016)
[3] F.D. Malone *et al.*, Phys. Rev. Lett. **117**, 115701 (2016) [4] T. Schoof *et al.*, Phys. Rev. Lett. (2015)

Ab initio dynamic (ω-dependent) results for the warm dense UEG

- **Key quantity:** dynamic structure factor

$$S(\mathbf{q},\omega) := \frac{1}{2\pi}\int_{-\infty}^{\infty} \mathrm{d}t \underbrace{\langle \hat{n}_{\mathbf{q}}(t)\hat{n}_{-\mathbf{q}}(0)\rangle}_{:=F(\mathbf{q},t)} e^{i\omega t}$$

$\rightarrow$ Directly measured in **scattering experiments**

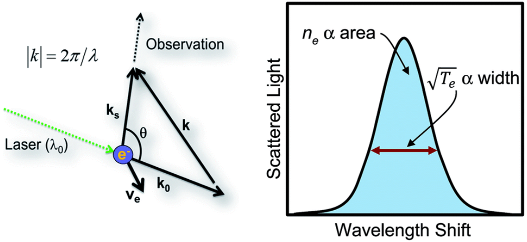

X-ray Thomson scattering experiments at free electron laser facilities (e.g. FLASH, X-FEL, LCLS)

yields the most accurate information on plasma density, ionic charge state, and temperature

Analysis requires model input

Ab initio dynamic (ω-dependent) results for the warm dense UEG

- **Key quantity:** dynamic structure factor

$$S(\mathbf{q},\omega) := \frac{1}{2\pi}\int_{-\infty}^{\infty} \mathrm{d}t\, \underbrace{\langle \hat{n}_{\mathbf{q}}(t)\hat{n}_{-\mathbf{q}}(0)\rangle}_{:=F(\mathbf{q},t)}\, e^{i\omega t}$$

$\rightarrow$ Directly measured in **scattering experiments**

- **Chihara decomposition** applies for non-collective scattering:

$$S(\mathbf{q},\omega) = S_{\text{b-b}}(\mathbf{q},\omega) + S_{\text{b-f}}(\mathbf{q},\omega) + S_{\text{f-f}}(\mathbf{q},\omega)$$

$$\rightarrow S_{\text{f-f}}(\mathbf{q},\omega) \sim S^{\text{UEG}}(\mathbf{q},\omega)$$

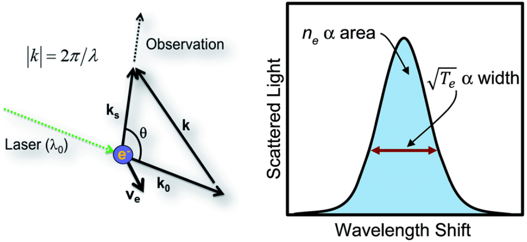

X-ray Thomson scattering experiments at free electron laser facilities (e.g. FLASH, X-FEL, LCLS)

yields the most accurate information on plasma density, ionic charge state, and temperature

Analysis requires model input

Ab initio dynamic (ω-dependent) results for the warm dense UEG

- **Key quantity:** dynamic structure factor

$$S(\mathbf{q},\omega) := \frac{1}{2\pi}\int_{-\infty}^{\infty} \mathrm{d}t \underbrace{\langle \hat{n}_{\mathbf{q}}(t)\hat{n}_{-\mathbf{q}}(0)\rangle}_{:=F(\mathbf{q},t)} e^{i\omega t}$$

$\rightarrow$ Directly measured in **scattering experiments**

- **Chihara decomposition** applies for non-collective scattering:

$$S(\mathbf{q},\omega) = S_{\text{b-b}}(\mathbf{q},\omega) + S_{\text{b-f}}(\mathbf{q},\omega) + S_{\text{f-f}}(\mathbf{q},\omega)$$

$$\rightarrow S_{\text{f-f}}(\mathbf{q},\omega) \sim S^{\text{UEG}}(\mathbf{q},\omega)$$

- **Practical example:** Fit model for $S(\mathbf{q},\omega;T_e)$ to spectrum to determine electron temperature T_e

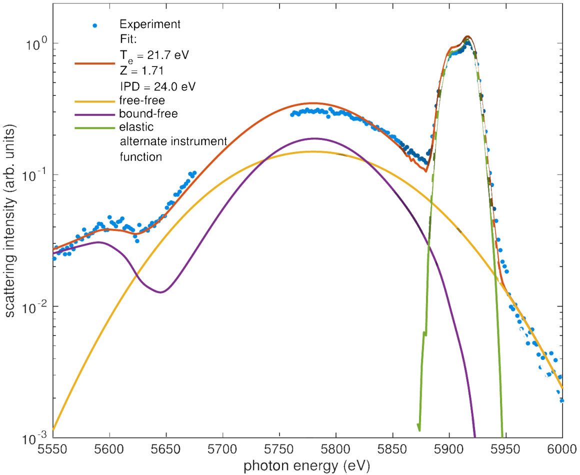

Scattering spectrum of isochorically heated graphite at LCLS. From D. Kraus *et al.*, *Plasma Phys. Control. Fusion* (2019)

Ab initio dynamic (ω-dependent) results for the warm dense UEG

- **Key quantity:** dynamic structure factor

$$S(\mathbf{q},\omega) := \frac{1}{2\pi}\int_{-\infty}^{\infty} \mathrm{d}t \underbrace{\langle \hat{n}_{\mathbf{q}}(t)\hat{n}_{-\mathbf{q}}(0)\rangle}_{:=F(\mathbf{q},t)} e^{i\omega t}$$

  $\rightarrow$ Directly measured in **scattering experiments**

- **Chihara decomposition** applies for non-collective scattering:

$$S(\mathbf{q},\omega) = S_{\text{b-b}}(\mathbf{q},\omega) + S_{\text{b-f}}(\mathbf{q},\omega) + S_{\text{f-f}}(\mathbf{q},\omega)$$

$$\rightarrow S_{\text{f-f}}(\mathbf{q},\omega) \sim S^{\text{UEG}}(\mathbf{q},\omega)$$

- **Practical example:** Fit model for $S(\mathbf{q},\omega;T_e)$ to spectrum to determine electron temperature T_e
- **Problem:**
  $F(\mathbf{q},t)$ requires **real time-dependent simulations**
  $\rightarrow$ with PIMC have to use analytic continuation, reconstruct $F(q,it)$ and 4 frequency moments, but: insufficient information

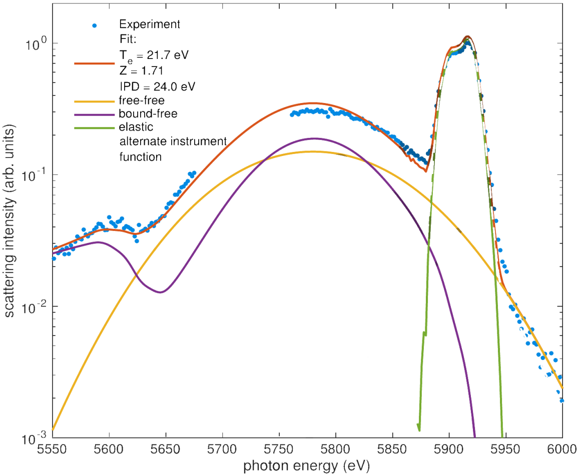

Scattering spectrum of isochorically heated graphite at LCLS.
From D. Kraus *et al.*, *Plasma Phys. Control. Fusion* (2019)

Incorporating additional information on $S(\mathbf{q}, \omega)$ via dielectric formulation

- **Fluctuation-dissipation theorem:**

$$S(\mathbf{q}, \omega) = -\frac{\mathrm{Im}\chi(\mathbf{q}, \omega)}{\pi n(1 - e^{-\beta\omega})}$$

Dynamic structure factor of the UEG:
($\theta = 1$, $r_s = 10$, $N = 33$, $q = 0.63 q_F$)

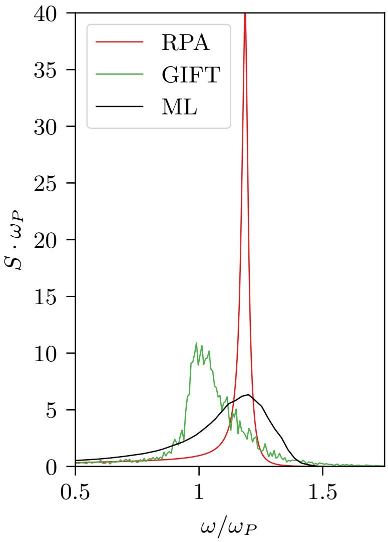

Incorporating additional information on $S(\mathbf{q},\omega)$ via dielectric formulation

- **Fluctuation-dissipation theorem:**

$$S(\mathbf{q},\omega) = -\frac{\mathrm{Im}\chi(\mathbf{q},\omega)}{\pi n(1-e^{-\beta\omega})}$$

- Express response function χ via ideal response function χ_0 and **dynamic local field correction** G:

$$\chi(\mathbf{q},\omega) = \frac{\chi_0(\mathbf{q},\omega)}{1 - v_q\left[1 - G(\mathbf{q},\omega)\right]\chi_0(\mathbf{q},\omega)}$$

- **Random phase approximation (RPA):** $G \equiv 0$

Dynamic structure factor of the UEG:
($\theta = 1$, $r_s = 10$, $N = 33$, $q = 0.63q_F$)

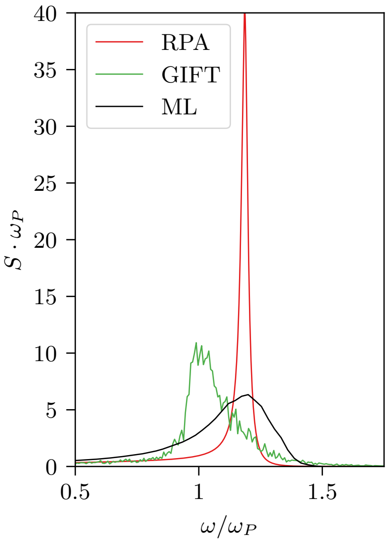

Incorporating additional information on $S(\mathbf{q},\omega)$ via dielectric formulation

- **Fluctuation-dissipation theorem:**

$$S(\mathbf{q},\omega) = -\frac{\mathrm{Im}\chi(\mathbf{q},\omega)}{\pi n(1-e^{-\beta\omega})}$$

- Express response function χ via ideal response function χ_0 and **dynamic local field correction** G:

$$\chi(\mathbf{q},\omega) = \frac{\chi_0(\mathbf{q},\omega)}{1 - v_q\left[1 - G(\mathbf{q},\omega)\right]\chi_0(\mathbf{q},\omega)}$$

- **Random phase approximation (RPA):** $G \equiv 0$

Make ansatz and optimize $G(\mathbf{q},\omega)$ instead of $S(\mathbf{q},\omega)$

Advantages:

- Limits $G(\mathbf{q},0)$ and $G(\mathbf{q},\infty)$ known from PIMC simulation
- Other exact properties of G can be incorporated

Dynamic structure factor of the UEG:
($\theta = 1$, $r_s = 10$, $N = 33$, $q = 0.63q_F$)

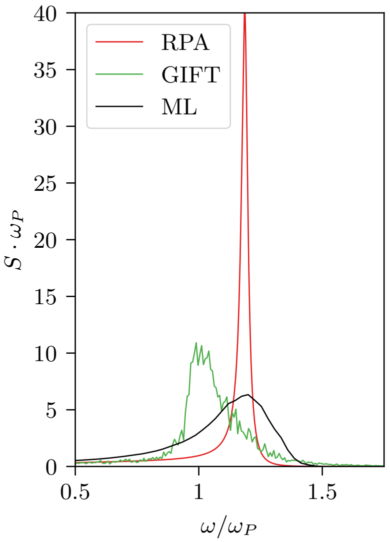

Incorporating additional information on $S(\mathbf{q},\omega)$ via dielectric formulation

- **Fluctuation-dissipation theorem:**

$$S(\mathbf{q},\omega) = -\frac{\mathrm{Im}\chi(\mathbf{q},\omega)}{\pi n(1-e^{-\beta\omega})}$$

- Express response function χ via ideal response function χ_0 and **dynamic local field correction** G:

$$\chi(\mathbf{q},\omega) = \frac{\chi_0(\mathbf{q},\omega)}{1 - v_q\left[1 - G(\mathbf{q},\omega)\right]\chi_0(\mathbf{q},\omega)}$$

- **Random phase approximation (RPA):** $G \equiv 0$

Make ansatz and optimize $G(\mathbf{q},\omega)$ instead of $S(\mathbf{q},\omega)$

Advantages:

- Limits $G(\mathbf{q},0)$ and $G(\mathbf{q},\infty)$ known from PIMC simulation
- Other exact properties of G can be incorporated

Dynamic structure factor of the UEG:
($\theta = 1$, $r_s = 10$, $N = 33$, $q = 0.63q_F$)

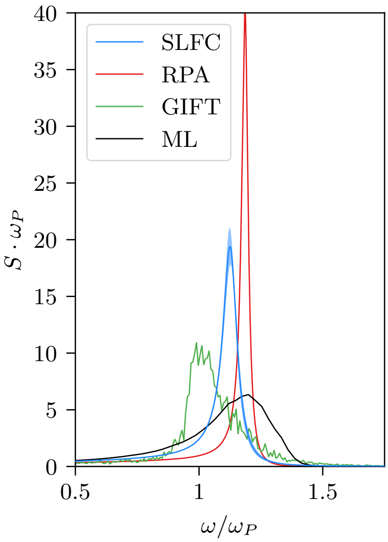

Incorporating additional information on $S(\mathbf{q},\omega)$ via dielectric formulation

- **Fluctuation-dissipation theorem:**

$$S(\mathbf{q},\omega) = -\frac{\mathrm{Im}\chi(\mathbf{q},\omega)}{\cdots}$$

- Ex…
  dy…

GIFT and ML spectra not in agreement with exact properties of $G(\mathbf{q},\omega)$
$\rightarrow$ to be discarded as unphysical

$$\chi(\mathbf{q},\omega) = \frac{\cdots}{1 - v_q\left[1 - G(\mathbf{q},\omega)\right]\chi_0(\mathbf{q},\omega)}$$

- **Random phase approximation (RPA):** $G \equiv 0$

Make ansatz and optimize $G(\mathbf{q},\omega)$ instead of $S(\mathbf{q},\omega)$

Advantages:

- Limits $G(\mathbf{q},0)$ and $G(\mathbf{q},\infty)$ known from PIMC simulation
- Other exact properties of G can be incorporated

Dynamic structure factor of the UEG:
($\theta = 1$, $r_s = 10$, $N = 33$, $q = 0.63q_F$)

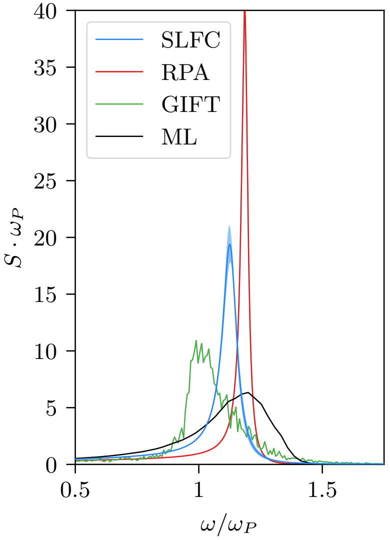

Incorporating additional information on $S(\mathbf{q},\omega)$ via dielectric formulation

- **Fluctuation-dissipation theorem:**

$$S(\mathbf{q},\omega) = -\frac{\mathrm{Im}\chi(\mathbf{q},\omega)}{\quad}$$

- Ex
dy

GIFT and ML spectra not in agreement with exact properties of $G(\mathbf{q},\omega)$
$\rightarrow$ to be discarded as unphysical

$$\chi(\mathbf{q},\omega) = \frac{\quad}{1 - v_q\left[1 - G(\mathbf{q},\omega)\right]\chi_0(\mathbf{q},\omega)}$$

- **Random phase approximation (RPA):** $G \equiv 0$

Stochastic sampling of $G(\mathbf{q},\omega)$ accurately determines $S(\mathbf{q},\omega)$

Advantages:

- Limits $G(\mathbf{q},0)$ and $G(\mathbf{q},\infty)$ known from PIMC simulation
- Other exact properties of G can be incorporated

Dynamic structure factor of the UEG:
($\theta = 1$, $r_s = 10$, $N = 33$, $q = 0.63q_F$)

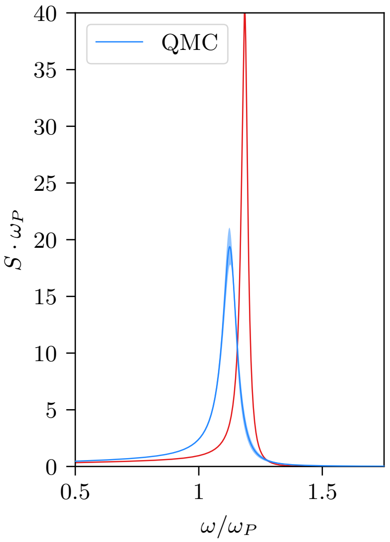

Correlation effects in the peak position of $S(q, \omega)$: $\theta = 1$, $r_s = 2$

T. Dornheim, S. Groth, J. Vorberger, and M. Bonitz, *Phys. Rev. Lett.* **121**, 255001 (2018)

- *Ab initio* results for $G(q, 0)$ available: Dornheim *et al.*, J. Chem. Phys. (2019)
- Slight **correlation induced redshift** of peak for intermediate q (at small r_s)

Dynamic structure factor of the UEG:

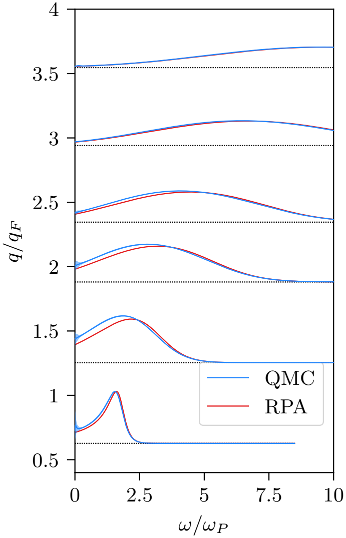

Peak position and FWHM:

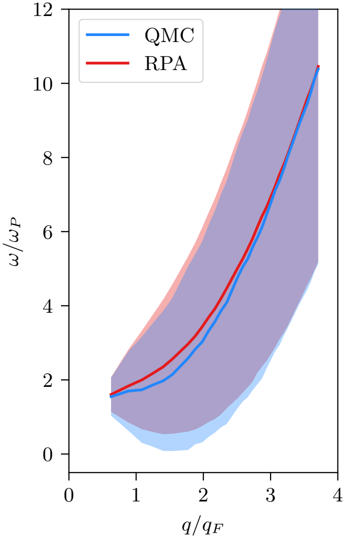

Correlation effects in the peak position of $S(q,\omega)$: $\theta = 1$, $r_s = 6$

T. Dornheim, S. Groth, J. Vorberger, and M. Bonitz, *Phys. Rev. Lett.* **121**, 255001 (2018)

- *Ab initio* results for $G(q,0)$ available: Dornheim *et al.*, J. Chem. Phys. (2019)
- Slight **correlation induced redshift** of peak for intermediate q (at small r_s)
- **Pronounced redshift** and **broadening** with increasing r_s

Dynamic structure factor of the UEG:

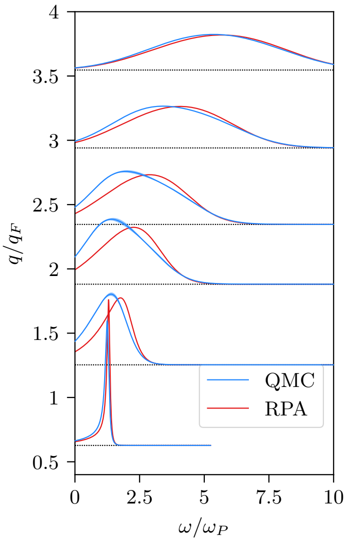

Peak position and FWHM:

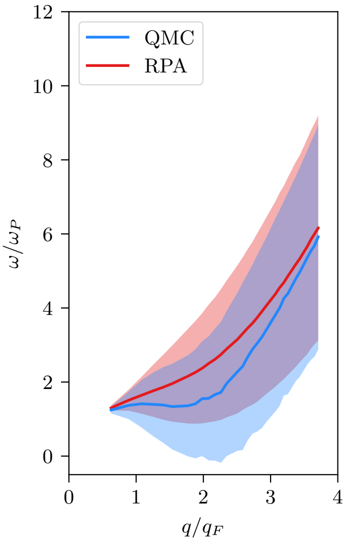

Correlation effects in the peak position of $S(q,\omega)$: $\theta = 1$, $r_s = 10$

T. Dornheim, S. Groth, J. Vorberger, and M. Bonitz, *Phys. Rev. Lett.* **121**, 255001 (2018)

- *Ab initio* results for $G(q,0)$ available: Dornheim *et al.*, J. Chem. Phys. (2019)
- Slight **correlation induced redshift** of peak for intermediate q (at small r_s)
- **Pronounced redshift** and **broadening** with increasing r_s
- **Negative dispersion of peak** for large r_s around $q = 2q_F$ **predicted for dense hydrogen**
- **How is this related to plasmons?**

  Requires dielectric function $\epsilon(q,\omega)$

$$S(\mathbf{q},\omega) = -\frac{\operatorname{Im}\epsilon^{-1}(\mathbf{q},\omega)}{\pi n\tilde{v}(q)(1-e^{-\beta\omega})}$$

Dynamic structure factor of the UEG:

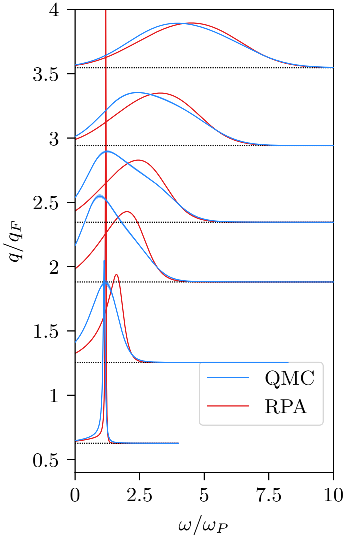

Peak position and FWHM:

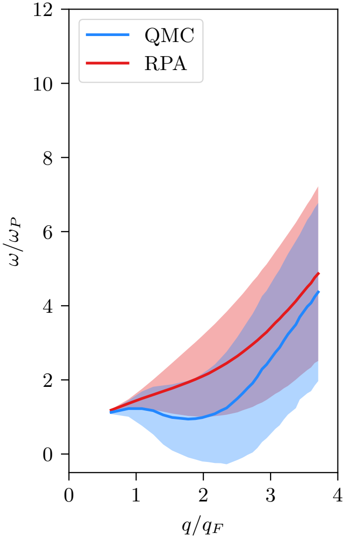

WDM Dielectric function: finite temperature, quantum and correlation effects

- Quantum hydrodynamics[2]: incorrect plasmon dispersion in 2D and 3D (factor $9/5$ in q^2 term)[3]
- Quantum Vlasov (Hartree, mean field or random phase) approximation (RPA) at finite T:

$$\epsilon(q,\omega;T) = 1 - \tilde{v}(q)\Pi(q,\omega;T)\,, \quad \Pi^{\mathrm{RPA}}(\vec{q},\omega;T) = \int \frac{d\vec{p}}{(2\pi)^3} \frac{f\left(E_{\vec{p}};T\right) - f\left(E_{\vec{p}+\vec{q}};T\right)}{E_{\vec{p}} - E_{\vec{p}+\vec{q}} + \omega + i\delta}\,, \qquad \delta \to 0^+\,.$$

- Mean field plus correlations: models for local field correction $G(q,\omega)$ or quantum kinetic theory:

$$\Pi^{\mathrm{RPA}} \to \Pi(q,\omega) = \frac{\Pi^{\mathrm{RPA}}(q,\omega)}{1 + \tilde{v}(q)G(q,\omega)\Pi^{\mathrm{RPA}}(q,\omega)}\,.$$

- Exact results[4] : $G^{\mathrm{QMC}}(q,\omega) \to \Pi^{\mathrm{QMC}}(q,\omega) \to \epsilon^{\mathrm{QMC}}(q,\omega)$

  Accurate and efficient approximation: $G^{\mathrm{QMC}}(q,\omega) \to G^{\mathrm{QMC}}(q,0) = G(q)$, insert in $\Pi(q,\omega) \to \epsilon^{\mathrm{SLFC}}(q,\omega;T)$

- QHD with exchange-correlation corrections[5], but only: $T = 0$ and low accuracy xc effects (LDA)
- Improved QHD[6]: finite T, ω- and q-dependent coefficients, correlations via G and non-local effects

---

[2] G. Manfredi and F. Haas, Phys. Rev. B (2001)
[3] M. Bonitz *et al.*, Phys. Plasmas (2019)
[4] P. Hamann *et al.*, Phys. Rev. B (2020), arXiv: 2007.15471
[5] N. Crouseilles *et al.*, Phys. Rev. B (2008)
[6] Zh. Moldabekov *et al.*, Phys. Plasmas (2019)

Parametrizations of the plasmon dispersion of the 3D electron gas (mean field)

- Bohm and Gross 1949, classical plasma[7]: $\frac{\omega^2(q)}{\omega_p^2} = 1 + \frac{v_{th}^2}{\omega_p^2} q^2, \quad v_{th}^2 = \frac{3k_B T}{m}$
- Bohm and Pines 1953, quantum plasma, $T = 0$ (RPA)[8]: $\frac{\omega^2(q)}{\omega_p^2} = 1 + \frac{3}{5}\frac{v_F^2}{\omega_p^2} q^2 + \frac{\hbar^2}{4m^2}\frac{q^4}{\omega_p^2}$,
- Ferrell 1957, q^4 terms, $T = 0$[9]: $\frac{\omega^2(q)}{\omega_p^2} = 1 + \frac{3}{5}\frac{v_F^2}{\omega_p^2} q^2 + \left(\frac{(\Delta v_0^2)^2}{\omega_p^2} + \frac{\hbar^2}{4m^2}\right)\frac{q^4}{\omega_p^2}, \qquad \left(\Delta v_0^2\right)^2 = \langle v^4\rangle_0 - \langle v^2\rangle_0^2$
- Quantum hydrodynamics ($T = 0$)[10]: $\frac{\omega^2(q)}{\omega_p^2} = 1 + \frac{1}{3}\frac{v_F^2}{\omega_p^2} q^2 + \frac{\hbar^2}{4m^2}\frac{q^4}{\omega_p^2}$,
- Hamann *et al.*[11] RPA, finite T : $\frac{\omega^2(q)}{\omega_p^2} = 1 + \frac{\langle v^2\rangle}{\omega_p^2} q^2 + \left(\frac{(\Delta v^2)^2}{\omega_p^2} + \frac{\hbar^2}{4m^2}\right)\frac{q^4}{\omega_p^2}, \quad \langle \dots \rangle$ average with Fermi function

Analytical parametrization for WDM: $\frac{\omega^2(q)}{\omega_p^2} = 1 + B_2(r_s, \Theta)\frac{q^2}{q_F^2} + B_4(r_s, \Theta)\frac{q^4}{q_F^4}$

Note: finite q-range of plasmons to be accounted for separately

[7] D. Bohm and E.P. Gross, Phys. Rev. (1949)
[8] D. Bohm and D. Pines, Phys. Rev. (1953), also: Lindhard, Klimontovich, Silin
[9] R.A. Ferrell, Phys. Rev. (1957)
[10] G. Manfredi and F. Haas, Phys. Rev. B (2001)
[11] P. Hamann et al., Contrib. Plasma Phys. (2020), arXiv: 2008.04605

Dielectric function: plasmons

- Solution of Maxwell's equations: EM field modes, $E(q,t)$, in plasma (isotropic), from

$$\hat{\epsilon}(\vec{q}, \omega(q)) = 0$$

- contains collective excitations (plasmon)
- weak damping approximation (WDA):

$$\mathrm{Re}\,\hat{\epsilon}(\vec{q}, \omega(q)) = 0$$

- roots on real axis vanish for $q \geq q_{\mathrm{cr}}$, and damping, $|\mathrm{Im}\,\omega|$, becomes large
- drop WDA and find exact roots

$$\hat{\epsilon}(\vec{q}, z) = 0$$

at complex frequencies $z = \omega - i\gamma$:

$$E(q;t) \sim e^{i\omega(q)t} e^{-\gamma(q)t}, \quad \gamma > 0$$

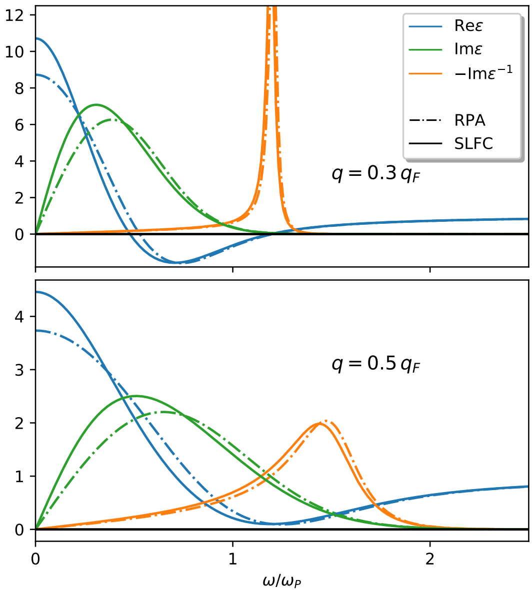

Figure: Moderately correlated electron gas, $\Theta = 1$, $r_s = 2$

Analytic continuation (AC) of the dielectric function[12]

- AC of the retarded DF into the lower frequency half plane, $\gamma > 0$.
- full lines: Re $\epsilon = 0$,
  dotted lines: Im $\epsilon = 0$,
  plasmon = intersection (arrows)
- green: mean field (RPA)
  black: correlated (static LFC)
- complex zeroes may exist, even if Re ϵ has no zeroes on real axis (top right).
- Finite temperature, $\Theta = 1$ ($k_B T = E_F$)

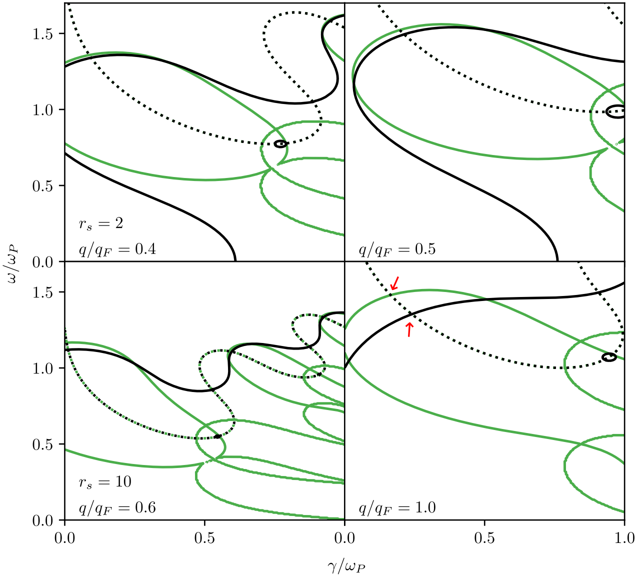

[12] M. Bonitz, Quantum Kinetic Theory, 2nd ed. Springer 2016; P. Hamann *et al.*, Contrib. Plasma Phys. (2020), arXiv:2008.04605

Plasmon dispersion in RPA: weak damping approximation vs. complex solution

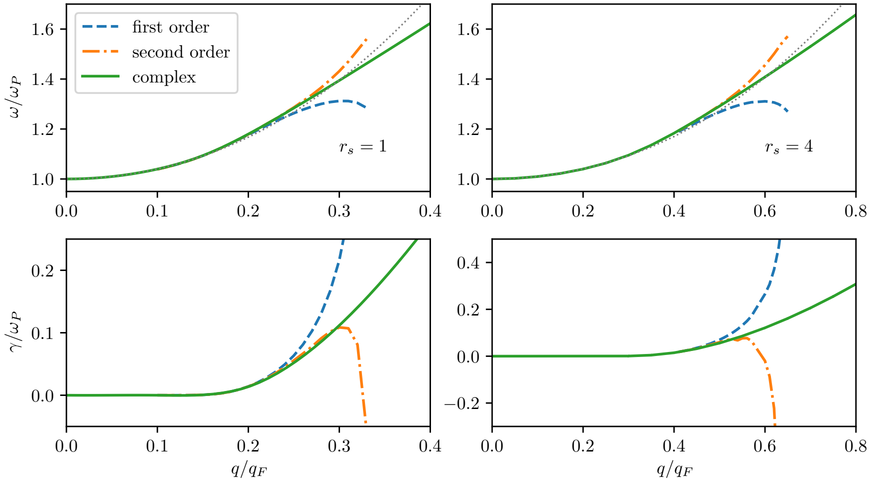

Figure: RPA-plasmon dispersion (top) and damping (bottom) for $\theta = 1$ and $r_s = 1$ (left) and $r_s = 4$ (right). Green line: complex dispersion; blue dashes: small damping approximation; dash-dotted orange: next order expansion result. Dots: analytical RPA parametrization. The complex dispersion solution exists up to about $q/q_F \approx 1.0$, for $r_s = 1$ and $q/q_F \approx 2.0$, for $r_s = 4$. From P. Hamann *et al.*, Contrib. Plasma Phys. (2020), arXiv:2008.04605

Plasmon dispersion for $\Theta = 0.5$

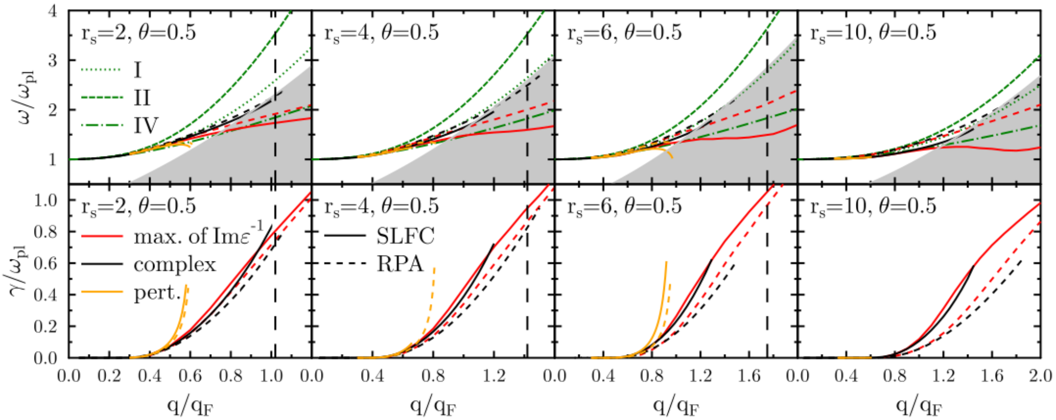

Figure: Plasmon dispersion (top) and damping (bottom) with (SLFC) and without (RPA) correlations. Orange: weak damping approximation. I: full RPA dispersion, II: $(\Delta v^2)^2$ replaced by $\langle v^4 \rangle$. IV: neglecting q^4-terms. Grey area: pair continuum. Vertical dashes: $q = \lambda_{\rm scr}$.From P. Hamann *et al.*, Contrib. Plasma Phys. (2020), arXiv:2008.04605

Plasmon dispersion for $\Theta = 2$

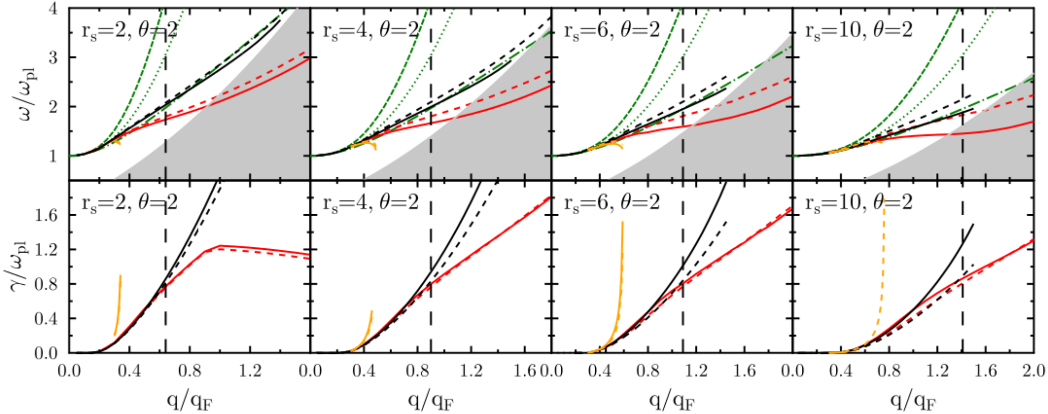

Figure: Plasmon dispersion (top) and damping (bottom) with (SLFC) and without (RPA) correlations. Orange: weak damping approximation. green dots: full RPA dispersion, green dashes: $(\Delta v^2)^2$ replaced by $\langle v^4 \rangle$. green dash-dots: neglecting q^4-terms. Red: peak of Im ϵ^{-1}, Grey area: pair continuum. Vertical dashes: $q = \lambda_{\rm scr}$. From P. Hamann *et al.*, Contrib. Plasma Phys. (2020), arXiv:2008.04605

Plasmon dispersion vs. Dynamics structure factor, for $\Theta = 1$

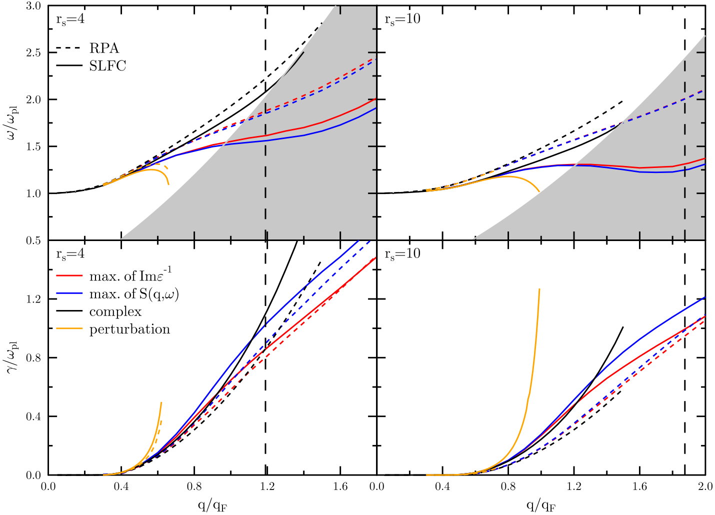

Figure: Plasmon dispersion (top) and damping (bottom) with (SLFC) and without (RPA) correlations. Orange: weak damping approximation. blue: peak of $S(q,\omega)$. Grey area: pair continuum. Vertical dashes: $q = \lambda_{\rm scr}$. From P. Hamann *et al.*, Contrib. Plasma Phys. (2020), arXiv:2008.04605

Summary[20]

- *ab initio* **QMC** simulations provide complete thermodynamic data for warm dense uniform electron gas[13]
- accurate functional $f_{\mathrm{xc}}(r_s, \Theta, \xi)$ input for finite-T LDA-DFT, implemented in Libxc (LDA_XC_GDSMFB)

- ab initio data for inhomogeneous EG[14] $\Rightarrow$ accurate parametrization of static local field correction[15] $G(q)$
- first *ab initio* data for the dynamic structure factor $S(q, \omega)$ and the dielectric function of warm dense electrons[16]
  first *ab initio* data for the plasmon dispersion $\omega(q)$, accurate parametrization[17]
- Direct comparison with state of the art Thomson scattering (XRTS) experiments possible

[13] T. Dornheim *et al.*, Phys. Reports (2018)
[14] S. Groth *et al.*, J. Chem. Phys. (2017); T. Dornheim *et al.*, Phys. Rev. E (2017)
[15] T. Dornheim et al., J. Chem. Phys. (2019)
[16] T. Dornheim *et al.*, Phys. Rev. Lett. (2018); P. Hamann *et al.*, Phys. Rev. B (2020), arXiv:2007.15471
[17] P. Hamann *et al.*, Contrib. Plasma Phys. (2020), arXiv:2008.04605
[18] Zh. Moldabekov *et al.*, Phys. Plasmas (2018); M. Bonitz *et al.*, Phys. Plasmas (2019)
[19] M. Bonitz, “Quantum Kinetic Theory”, 2nd ed. Springer 2016; N. Schlünzen *et al.*, J. Phys. Cond. Matt. **32**, 103001 (2020)
[20] http://www.theo-physik.uni-kiel.de/bonitz/index.html $\Rightarrow$ Research $\Rightarrow$ Publications, Talks

Summary[20]

- *ab initio* **QMC** simulations provide complete thermodynamic data for warm dense uniform electron gas[13]
- accurate functional $f_{\rm xc}(r_s, \Theta, \xi)$ input for finite-T LDA-DFT, implemented in Libxc (LDA_XC_GDSMFB)

- ab initio data for inhomogeneous EG[14] $\Rightarrow$ accurate parametrization of static local field correction[15] $G(q)$
- first *ab initio* data for the dynamic structure factor $S(q,\omega)$ and the dielectric function of warm dense electrons[16]
  first *ab initio* data for the plasmon dispersion $\omega(q)$, accurate parametrization[17]
- Direct comparison with state of the art Thomson scattering (XRTS) experiments possible

- **QHD** rigorously derived from Microscopic QHD (TDDFT), coefficients depend on excitation conditions [18]
  $\Rightarrow$ systematic improvements possible, promising for large space and time scales in WDM
  $\Rightarrow$ Focus on linear and nolinear plasmons in real XRTS experiments

---

[13] T. Dornheim *et al.*, Phys. Reports (2018)
[14] S. Groth *et al.*, J. Chem. Phys. (2017); T. Dornheim *et al.*, Phys. Rev. E (2017)
[15] T. Dornheim et al., J. Chem. Phys. (2019)
[16] T. Dornheim *et al.*, Phys. Rev. Lett. (2018); P. Hamann *et al.*, Phys. Rev. B (2020), arXiv:2007.15471
[17] P. Hamann *et al.*, Contrib. Plasma Phys. (2020), arXiv:2008.04605
[18] Zh. Moldabekov *et al.*, Phys. Plasmas (2018); M. Bonitz *et al.*, Phys. Plasmas (2019)
[19] M. Bonitz, "Quantum Kinetic Theory", 2nd ed. Springer 2016; N. Schlünzen *et al.*, J. Phys. Cond. Matt. **32**, 103001 (2020)
[20] http://www.theo-physik.uni-kiel.de/bonitz/index.html $\Rightarrow$ Research $\Rightarrow$ Publications, Talks

Summary[20]

- *ab initio* **QMC** simulations provide complete thermodynamic data for warm dense uniform electron gas[13]
- accurate functional $f_{\rm xc}(r_s, \Theta, \xi)$ input for finite-T LDA-DFT, implemented in Libxc (LDA_XC_GDSMFB)
- ab initio data for inhomogeneous EG[14] $\Rightarrow$ accurate parametrization of static local field correction[15] $G(q)$
- first *ab initio* data for the dynamic structure factor $S(q, \omega)$ and the dielectric function of warm dense electrons[16]
  first *ab initio* data for the plasmon dispersion $\omega(q)$, accurate parametrization[17]
- Direct comparison with state of the art Thomson scattering (XRTS) experiments possible
- **QHD** rigorously derived from Microscopic QHD (TDDFT), coefficients depend on excitation conditions [18]
  $\Rightarrow$ systematic improvements possible, promising for large space and time scales in WDM
  $\Rightarrow$ Focus on linear and nolinear plasmons in real XRTS experiments
- Electronic correlations and correlation build up (thermalization, dynamical screening, Auger processes etc.) are captured by (Nonequilibrium) **Green functions**. Highly efficient new computational techniques available[19]

---

[13] T. Dornheim *et al.*, Phys. Reports (2018)
[14] S. Groth *et al.*, J. Chem. Phys. (2017); T. Dornheim *et al.*, Phys. Rev. E (2017)
[15] T. Dornheim et al., J. Chem. Phys. (2019)
[16] T. Dornheim *et al.*, Phys. Rev. Lett. (2018); P. Hamann *et al.*, Phys. Rev. B (2020), arXiv:2007.15471
[17] P. Hamann *et al.*, Contrib. Plasma Phys. (2020), arXiv:2008.04605
[18] Zh. Moldabekov *et al.*, Phys. Plasmas (2018); M. Bonitz *et al.*, Phys. Plasmas (2019)
[19] M. Bonitz, “Quantum Kinetic Theory”, 2nd ed. Springer 2016; N. Schlünzen *et al.*, J. Phys. Cond. Matt. **32**, 103001 (2020)
[20] http://www.theo-physik.uni-kiel.de/bonitz/index.html $\Rightarrow$ Research $\Rightarrow$ Publications, Talks